Am. J. Hum. Genet. 66:1473–1484, 2000

Disruption of a Novel Imprinted Zinc-Finger Gene, *ZNF215,* in Beckwith-Wiedemann Syndrome

M. Alders,[1,2] A. Ryan,[3] M. Hodges,[3] J. Bliek,[1,2] A. P. Feinberg,[4] O. Privitera,[5] A. Westerveld,[1] P. F. R. Little,[3] and M. Mannens[1,2]

[1]Department of Human Genetics and [2]Department of Clinical Genetics, Academic Medical Center, Amsterdam; [3]Department of Biochemistry, Imperial College of Science, Technology and Medicine, London; [4]Department of Medicine, Johns Hopkins University School of Medicine, Baltimore; and [5]Laboratorio di Citogenetica, Azienda Ospedaliera di Legnano, Legnano, Italy

The genetics of Beckwith-Wiedemann syndrome (BWS) is complex and is thought to involve multiple genes. It is known that three regions on chromosome 11p15 (*BWSCR1, BWSCR2,* and *BWSCR3*) may play a role in the development of BWS. *BWSCR2* is defined by two BWS breakpoints. Here we describe the cloning and sequence analysis of 73 kb containing *BWSCR2.* Within this region, we detected a novel zinc-finger gene, *ZNF215.* We show that two of its five alternatively spliced transcripts are disrupted by both *BWSCR2* breakpoints. Parts of the 3′ end of these splice forms are transcribed from the antisense strand of a second zinc-finger gene, *ZNF214.* We show that *ZNF215* is imprinted in a tissue-specific manner.

Introduction

The Beckwith-Wiedemann syndrome (BWS) (MIM 130650) is characterized by a wide variety of growth abnormalities. Exomphalos, macroglossia, and gigantism—which are the most common features—are variably present and can be found in association with multiple anomalies such as hypoglycemia, ear pits and creases, and hemihypertrophy (Pettenati et al. 1986). BWS patients are prone to develop several embryonic tumors (7.5%), most commonly (40% of all tumors) Wilms tumor (WT) (MIM 194071) (Wiedemann 1983). Both linkage studies and the presence of chromosomal abnormalities assigned this syndrome to chromosome 11p15.5 (Koufos et al. 1989; Ping et al. 1989), containing, amongst others, the gene *IGF2.*

The molecular etiology of BWS is complex and involves genomic imprinting (Mannens et al. 1994). Only recently has it been possible to develop a hypothesis to explain some of its features. It is suggested that inheritance of two functional copies of the primarily paternally expressed *IGF2* gene results in overproduction of this fetal-growth factor and consequent changes to development of predominantly mesodermally derived tissues and organs. Evidence for this hypothesis comes from the observation of parent-of-origin effects in BWS where the disorder is sometimes associated with inheritance of two copies of *IGF2* via the paternal germline (paternal UPD and partial trisomies) (Weksberg et al. 1996 and references therein) and the observation that the majority of BWS patients show loss of imprinting of this gene (Weksberg et al. 1993; Reik et al. 1995; Brown et al. 1996; Joyce et al. 1997). More direct evidence for a role for *IGF2* in BWS comes from the phenotype of mice overexpressing or transgenic for *Igf2,* which exhibit BWS-like morphological changes (Sun et al. 1997; Eggenschwiler et al 1997).

A cluster of translocation breakpoints, contained within an ~300-kb interval 200–300 Kb proximal of *IGF2,* defines the BWS chromosome region 1 (*BWSCR1*) (Hoovers et al. 1995). *BWSCR1* is in the center of a region that contains multiple imprinted genes including *IGF2, H19, CDKN1C* (also known as *p57*[KIP2]), *ASCL2* (also known as *HASH2*), and *KCNQ1* (also known as *KVLQT1*). All breakpoints in *BWSCR1* disrupt the imprinted (maternally expressed) *KCNQ1* gene (Lee et al. 1997*b*). The involvement of *KCNQ1* in BWS and the effect of the translocations in this region on the imprinting and expression of the other candidate genes are not yet fully understood. In any event, in at least two patients, disruption of *BWSCR1* results in loss of imprinting (LOI) of *IGF2* (Brown et al. 1996; Smilinich et al. 1999).

Several observations suggest that disruption of *IGF2* imprinting is not the only process involved in the etiology of BWS. Recently, *LIT1,* an imprinted transcript antisense to *KCNQ1,* was identified. LOI of this paternally expressed transcript is observed in ~50% of the BWS patients and seems to be independent of LOI of *IGF2.* In addition, mutations in the preferentially maternally transcribed cell-cycle inhibitor *CDKN1C,* are

Received March 31, 1999; accepted for publication March 3, 2000; electronically published April 10, 2000.

Address for correspondence and reprints: Dr. M. M. A. M. Mannens, Department of Clinical Genetics, Meibergdreef 15, 1105 AZ Amsterdam, The Netherlands. E-mail: m.a.mannens@amc.uva.nl.

0002-9297/2000/6605-0002$02.00

found in a small subset of patients (Hatada et al. 1996; Okeefe et al. 1997; Lee et al. 1997*a*; authors' unpublished data) and the phenotype of mice null for *cdkn1c* had some similarities to BWS (Zhang et al. 1997; Yan et al. 1997). The exact molecular events associated with *BWSCR1* rearrangements and BWS remain to be established, but two additional regions of rearrangements add further complexity.

BWSCR2 and *BWSCR3* map, respectively, 5 Mb and 7 Mb more proximal to *BWSCR1* (Redeker et al. 1994). *BWSCR2* is defined by two breakpoints and may be associated with a distinct phenotype. Patient WH5.1 has hemihypertrophy and ear pits and grooves and has developed a Wilms tumor. Patient CRO2 presented with gigantism, cardiac abnormalities (dextrocardia, cardiomegaly, and septum defects), and hemihypertrophy and underwent hypoglycemic crisis. Thus, both patients have only minor BWS features—but both have hemihypertrophy, a feature not seen in patients with chromosomal breakpoints in *BWSCR1* and *BWSCR3*. Hemihypertrophy is associated with an increased risk for childhood tumors. It is frequently present in BWS patients with Wilms tumors (40%, compared with 12.5% in BWS patients without Wilms tumors) (Wiedemann 1983). DeBaun et al. (1998) suggest a 4.6-fold increased relative risk in such patients. Patient WH5.1 did indeed develop a Wilms tumor. As such, WH5.1 is the only BWS/hemihypertrophy patient carrying a balanced translocation that developed a childhood tumor.

The distance between the regions, the fact that they do not disrupt the same large imprinted region, and the phenotypic heterogeneity between the patients with breakpoints in the different regions make it seem unlikely that *cis*-acting DNA sequences are affected by *BWSCR2/3*. We would suggest that an alternative hypothesis could be that there is a gene(s) at *BWSCR2* and *BWSCR3* that interacts with some components of the *IGF2/BWSCR1* system and influences the BWS phenotype via this mechanism.

In this article, we describe the isolation of two zinc-finger genes at *BWSCR2*: *ZNF214* and *ZNF215*. Alternative splice variants of *ZNF215*, partially running antisense of *ZNF214*, are disrupted by the breakpoints. *ZNF215* is expressed preferentially from the maternal allele, whereas *ZNF214* is not imprinted. These data support a role for *ZNF215*, and possibly for *ZNF214*, in the etiology of BWS.

Material and Methods

Patient Material

Genomic DNA and high-resolution metaphase chromosomes were isolated from Epstein-Barr virus–transformed lymphoblastoid cell lines of patients WH5.1 (inv[11][p15.4;q22.2]) and CRO2 (t[10;11][p13;p15.4]).

Fluorescent In Situ Hybridization

Cosmids and YACs were labeled by nick-translation. Hybridization was performed on metaphase chromosomes, as described previously (Hoovers et al. 1992). Hybridization to linear DNA was performed according to Fidlerova et al. (1994).

Construction of a Cosmid Contig

YAC A39D9 was subcloned in cosmid vector Lawrist 4. All cosmids were fingerprinted to identify potential overlap with each other and other cosmids in a database to construct a contig, as described elsewhere (Ivens et al. 1994).

DNA Sequencing

Sequencing of plasmids and RACE products was performed using the ABI PRISM™ Dye Terminator Cycle Sequencing Ready Reaction Kit (PE Biosystems) and following manufacturer's recommended conditions. Reactions were run on an ABI 377 automatic sequencer (PE Biosystems).

Cosmids q25 and q27 were sequenced by the Sanger Centre in Cambridge using shotgun and directed approaches. Subsequent analysis of q25 and q27 sequence was carried out via the United Kingdom MRC Human Genome Project Resource Centre's Nucleotide Identify X (NIX) front-end World Wide Web software—which includes Grail, Fex, Hexon, MZEF, Genemark, Genefinder, and Blast software—either searching EMBL, TREMBL, Swissprot, sequence-tagged-site, and expressed-sequence-tag databases or predicting gene features de novo, as appropriate. The DNA fragment in between q25 and q27 was isolated by PCR using primers q27F (GACCTTAAGACACACCATG) and q25R (GCTTATGGATATCCAGCAG), cloned in pBluescript and sequenced.

Rapid Amplification of cDNA ends (RACE)

RACE reactions were performed using Clontech's Placenta Marathon Ready cDNA kit, according to the manufacturer's conditions. Gene-specific primers for *ZNF215* were: 5′ RACE, Zn4 ATGAACTTCGGCAGAAGGC and Zn2 GTCTCAGGAATGAAAGCC (nested); and 3′ RACE, Zn7 CCTTCAACCGGAGCTCCTC and ME1 TGCATACTCGAGATAAGTCCTG (nested). Gene-specific primers for *ZNF214* were: 5′ RACE, 835R1 ATTTGAAGATTTGAGCGCTGGGTA and 835R2 CCCTTACCACACTCATCACAC (nested); 3′ RACE, 833R1 GGGATTCAGTCAGCGTTCACAT and 833R2 CAATGTGCT-

AAGTGTGGTAAAGG (nested). PCR products were cloned in pUC18 using the Sureclone ligation kit (Promega).

Amplification of the ZNF215 *Alternative Transcripts*

cDNA was synthesized from 3 μg RNA using MMulV reverse transcriptase (Promega) and poly dT primer in 20 μl. 5 μl cDNA was used for PCR, using primers V3R (GACGGTAACTTTCATCAGAGC) and 215F1 (CATGACTCTGAGGCATCTCG) to amplify V3 and V1R and 215F1 to amplify V1,V4, and V5.

Green Fluorescent Protein Fusions

Full-length *ZNF215V1* cDNA was generated by subcloning the *Kpn*I-*Hin*dIII fragment from the 5′ RACE product and the *Hin*dIII-*Eco*RV fragment containing part of exon 7 from q25, into the *Kpn*I and *Eco*RV restriction site in pcDNA3. In order to clone the coding sequence in frame with GFP in pEGFP, *ZNF215V1* was amplified using primers with *Kpn*I and *Bam*HI linkers GAGGTACCGCTATCTCAAAACCTCGAA (F) and CAGGATCCATGAGATTTTATCCAGCA (R) and was cloned in pEGFPC1.

Full-length *ZNF214* cDNA was generated by subcloning the *Hae*III-*Kpn*I fragment from the 5′ RACE product and the *Kpn*I-*Avr*I fragment containing the zinc fingers isolated from q27 into the *Eco*RV-*Xba*I sites in pcDNA3. *ZNF214* was amplified using primers with *Bam*HI and *Xho*I linkers CAGGATCCGCAGTAACATTTGAAGATG (F) and GACTCGAGGTAAACTTTGATTAAAGCTG (R) and was cloned in pEGFPC1.

Hep3b cells and cos-7 cells were plated at 10% density and were grown for 8 h on microscopy slides in six-well plates. 2 μg plasmid DNA (*ZNF214*-pEGFPC1, *ZNF215V1*-pEGFPC1, and pEGFPC1 [control]) was transfected overnight in 1 ml serum-free medium and 10 μl lipofectin (GIBCO BRL). After transfection, the medium was refreshed and cells were grown for another 8 h. Then cells were fixed in 4% paraformaldehyde, were dehydrated in alcohol series, and were mounted in Vectashield (Vector Laboratories).

Determination of Genomic Imprinting

ZNF215.—Genomic DNA was amplified using primers 5PZ (GAACTGTTGGTGCTGGAAC) and 5P1 (TCTGGCACTTGATACTCTCT) RT-PCR was performed on RNA isolated from tissues of heterozygous individuals. cDNA was synthesized from 1 μg RNA using MMulV reverse transcriptase (promega) and the internal primer V1R (GTCTCAGGAATGAAAGCC) (V1) or V3R (GACGGTAACTTTCATCAGAGC) (V3) in 20 μl. 5 μl cDNA was used for PCR using primers V1R/5PZ or V3R/5PZ to amplify *ZNF215V1* and *ZNF215V3*, respectively. A nested PCR was performed on both using primers 5PZ and 5PR (TGCAGGGCATATCTTCATCT) to get the same fragments for both variants.

The PCR products were analyzed on a 12.5% nondenaturing AA gel and run at 5°C 600V, 25 mA for 3 hours on a genephor system (Amersham Pharmacia Biotech).

ZNF214.—Genomic DNA was amplified using primers 214F1 (GCTTTTATCTCACCATGGG) and 214R1 (TCTAAGGACTGCCAAGGC) RT-PCR was performed on RNA isolated from tissues of heterozygous individuals. cDNA was synthesized from 1μg RNA using MMulV reverse transcriptase (promega) and the internal primer 214R2 (CCATTGAATCTCTCAGTAGG) in 20 μl. 5 μl cDNA was used for PCR using primers 214F2 (TGGAAATTCCTGGATTCTTC) and 214R2. (semi-)Nested PCR was performed using primers 214F2 and 214R1. Sequencing was performed using Cy5-labeled primers on an ALFexpress automated sequencer (Amersham Pharmacia Biotech).

Mutation Analysis

DNA was isolated from peripheral blood lymphocytes of 32 BWS patients and 11 hemihypertrophy patients (all non-UPD cases). The coding regions of *ZNF214* and *ZNF215* were amplified by PCR (primers available on request). PCR products analyzed by SSCP on 12.5% nondenaturing polyacrylamide gels (Amersham Pharmacia Biotech) ran at 5°C and 15°C, as described in GeneGel Excel protocols (Amersham Pharmacia Biotech). DNA was stained using the Silver staining kit (Amersham Pharmacia Biotech). PCR products presenting abberant conformers were reamplified from genomic DNA and were sequenced in both directions by the fluorescent dideoxy chain–termination method on an ABI 377 sequencer (PE Biosystems).

Results

Construction of a Cosmid Contig over the Breakpoints

It has previously been shown that *BWSCR2* is located between D11S776 and HPX (Redeker et al. 1995). By screening a YAC library with cosmid e2378 (D11S776) we isolated YAC A39D9 that, by FISH analysis, overlapped the two breakpoints (data not presented). Cosmids subcloned from the YAC A39D9 were fingerprinted to identify potential overlap with each other and with other cosmids in the database (see Methods). We constructed a contig of 150 kb (fig. 1a) and the integrity of this contig was checked by hybridization on extended DNA (fig. 1c, d). Rearrangements in patients CRO2 and WH5.1 define *BWSCR2* and FISH analysis shows that the cosmid q27 spans the CRO2 breakpoint (fig. 1b). Southern blots of WH5.1 DNA probed with fragments

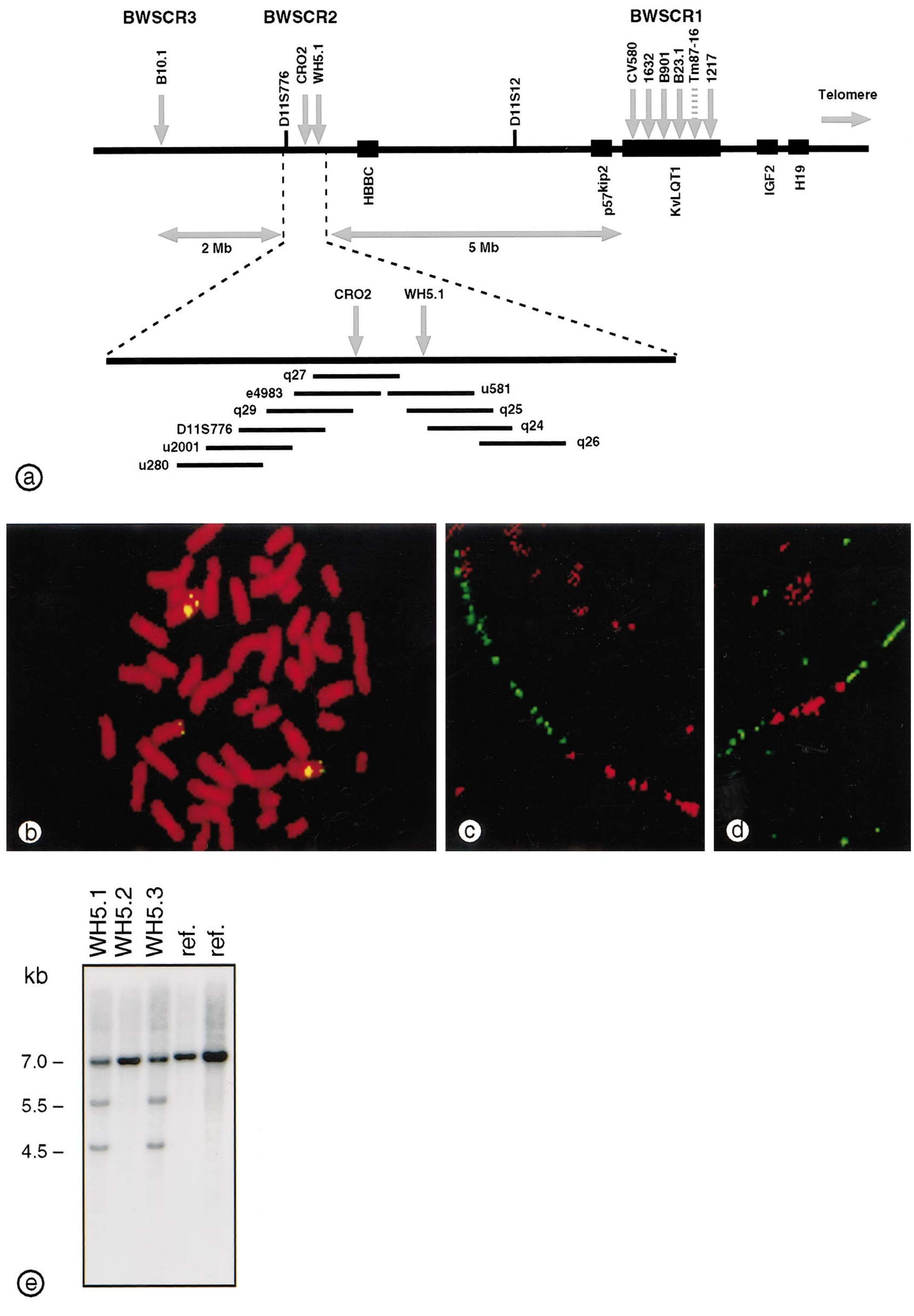

Figure 1 Localization of the breakpoints. *a,* Schematic map of chromosome 11p15. The three different breakpoint regions are indicated. The translocation breakpoint of the rhabdoid tumor Tm87-16 also maps within *BWSCR1*. The cosmid contig in *BWSCR2* is shown, as well as the localization of the breakpoints. *b,* Cosmid q27 hybridized to chromosomes of patient CRO2. Signals are visible on the normal 11, the derivative 11 and the derivative 10, indicating that this cosmid spans the breakpoint. *c,* FISH on linearized DNA, performed with cosmids q25 (red), q27 (green) and u280 (green) *d,* FISH on linearized DNA performed with cosmids q25 (green), q27 (red), and u280 (green). *e, Eco*RI digests of DNA derived from WH5.1, his father (WH5.2), his mother (WH5.3), and reference patients, hybridized with a fragment derived from q25. Two aberrant bands are detected in WH5.1 and WH5.3, indicating that this 7-kb *Eco*RI fragment contains the breakpoint.

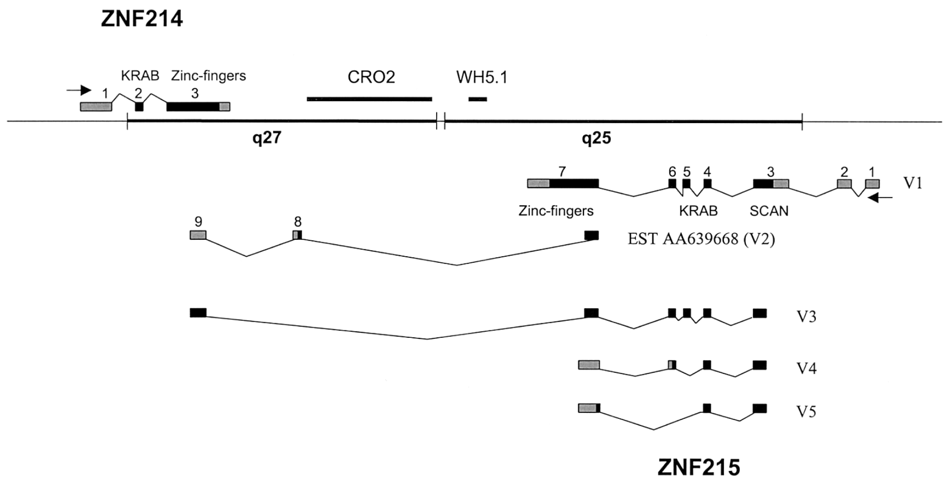

Figure 2 Schematic representation of the *BWSCR2* region. The breakpoint WH5.1 could be localized to a 1138-bp *Taq*I fragment. The position of CRO2 is not precisely mapped and is thought to be located in the last 15 kb of q27. Cosmids q25 and q27 were completely sequenced, allowing precise mapping of the exons of *ZNF214* and *ZNF215* in this region. Exons 3–7, covering the coding part of *ZNF215*, are present in cosmid q25; alternative exons 8 and 9 are present in cosmid q27. Exons 2 and 3 of *ZNF214* were found at the centromeric end of q27. Exon 1 maps outside q27, and its localization is not yet known. The coding regions of the genes are stained black, and the 3′ UTRs and 5′ UTRs are depicted in gray.

derived from q25 showed that the breakpoint mapped to a ~7-kb *Eco*RI fragment (fig. 1e). Additional experiments refined this localization to a 1138-bp *Taq*I fragment (data not shown).

Zinc-Finger Genes Are Associated with BWSCR2

In a previous study (Hoovers et al. 1992), we demonstrated that cosmid e2378, that contains D11S776, contains zinc-finger motifs. The presence of this cosmid in the contig that overlaps the breakpoints led us to search for other zinc-finger motifs in this region, using a degenerate oligo coding for the conserved C_2H_2-zinc-finger linker sequence HTGEKPY. Positive signals were observed in e2378 and in overlapping cosmids, and in q25, q24, and cSRL7e1. The positive fragments were subcloned and sequenced, and zinc-finger motifs were detected. Subsequently, we identified these motifs as being derived from two zinc-finger genes, *ZNF214* and *ZNF215,* respectively encoded in q27 and q25. These observations suggested there might be zinc-finger–coding genes disrupted by the breakpoints in patients CRO2 and WH5.1. We therefore sequenced cosmids q25 and q27 to determine whether this was the case.

Sequence Analysis

Cosmids q27 and q25 were completely sequenced by the Sanger Centre. The 686-bp gap between q25 and q27 subsequently was isolated by use of PCR (see Material and Methods) and also were sequenced, which led to a 73-kb continuous sequence. Separately, the zinc-finger sequences generated from q27 and q25 were used to screen cDNA libraries and to carry out RACE to isolate cDNAs for both genes. Extensive computer analysis (see Methods) of the cosmids detected only the two zinc-finger genes—*ZNF214* and *ZNF215*—and, among others, an EST (AA639668) mapping to the region.

Analysis of the complete sequences of the two cosmids and comparison to the cDNA sequences enabled us to show that *ZNF214* is located at the proximal end of q27 and transcription is towards the telomere; *ZNF215* is located towards the proximal end of q25 and is transcribed towards the centromere: *ZNF214* and *ZNF215* are therefore transcribed convergently. The exon 1 of *ZNF214* is not contained in q27: exon 2 is at 371–517 and exon 3 at 1671–3920. Three ESTs were found that run until 4695 or 5046, and probably represent transcripts that use alternative polyadenylation sites. Similarly, exons 1 and 2 of *ZNF215* are encoded outside of q25; exon 3 is at 32721–32143, exon 4 at 23241–23157, exon 5 at 21729–21597, exon 6 at 21266–21171, and exon 7 at 9123–6767.

EST AA639668 contains part of exon 7 of *ZNF215* (9123–9031), and two novel exons: 8 (at 14997–14903 in q27) and 9 (at 2532–2205 in q27). The latter runs antisense of *ZNF214* (fig. 2). This suggests that *ZNF215* is alternatively spliced, and this was tested by RT-PCR experiments making use of (1) primers derived from exon 3 and exon 9 and (2) mRNA from fibroblasts and the hepatoma cell-line Hep3B (fig. 3). Sequence analysis of resulting products showed that an mRNA was produced that contained exons 3, 4, 5, 6, 7, and 9, but not exon 8 (V3 in fig. 2). Additional RT-PCR experiments

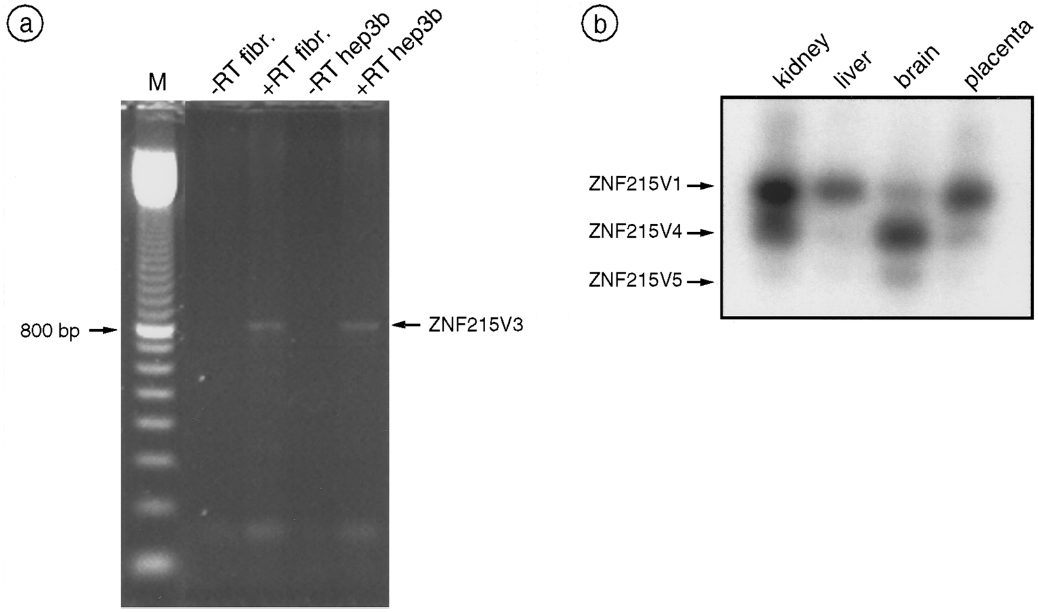

Figure 3 Alternative transcripts of *ZNF215. a,* RT-PCR performed on fibroblasts and Hep3b RNA, using primers derived from exon 9 and exon 3. An 831-bp fragment is produced, representing *ZNF215V3. b,* Tissue-specific expression of the *ZNF215V4* and *ZNF215V5* splice variants. Kidney, liver, and placenta express predominantly the *ZNF215V1* RNA. The smaller variants, *ZNF215V4* and *ZNF215V5* are expressed in brain tissue. This was reproducible in three more brain samples and two more kidney samples (data not shown).

also revealed the presence of two additional splice forms, V4 and V5, which lack exon 5 and exons 5 and 6, respectively (fig. 2). These splice variants show a tissue-specific expression pattern (fig. 3). In general, both *ZNF214* and *ZNF215V1* are widely expressed at very low levels by northern analyses. Expression is highest in the testis (data not shown). *ZNF215V2–ZNF215V5* are not detectable on northern blots, but they can be amplified by RT-PCR from several fetal and adult tissues.

ZNF214 and ZNF215 Proteins

ZNF214 (fig. 4a) contains 12 zinc fingers—of which fingers 1, 2, and 4 lack a cysteine, whereas fingers 2 and 4, respectively, lack a leucine and a phenylalanine residue in the consensus finger sequence, C X_2 C X_3 F X_5 L X_2 H X_3 H. At the N-terminal ZNF214 contains a KRABA domain. ZNF215 (fig. 4b) contains four zinc fingers, which are present in two pairs of two, with a small spacer in between. ZNF215 contains a KRABA domain; similarities to a KRABB domain; and, at the amino-terminal, a SCAN box. A nuclear localization signal, KKKR, was also present. In the variants represented by *ZNF215V3* and EST AA639668 (V2), the alternative splicing in exon 7 leads to truncated proteins consisting of only the SCAN box and KRAB domain and excluding the zinc fingers. In the *ZNF215V3* variant, lacking exon 8, the open reading frame continues coding for 98 additional amino acids. In variants *ZNF215V4* and *ZNF215V5,* the alternative splicing causes a frameshift, allowing only the synthesis of the SCAN box.

Zinc-finger proteins that are involved in transcription regulation exert their function in the nucleus. If ZNF214 and ZNF215 were involved in transcriptional regulation, in the most general sense, we would expect them to be located in the nucleus. We tested this by fusing the V1 cDNA of *ZNF215* and the full-length cDNA of *ZNF214* to the green fluorescent protein (GFP) in p-EGFPC1. Transfection of these constructs to cos-7 or Hep3b cells showed that, after 24 h, both ZNF214 and ZNF215 are present in the nucleus. Transfection of the control construct, the empty *pEGFPc1* vector, led to

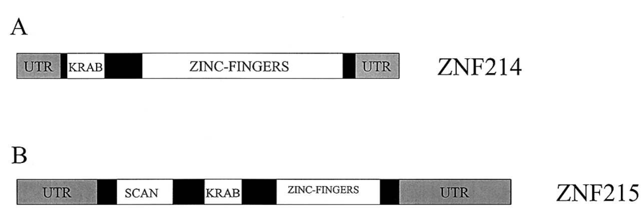

Figure 4 *a,* Schematic representation of the *ZNF214* gene. The KRAB domain and the zinc-finger region are indicated. *b,* Schematic representation of the *ZNF215V1* gene. The SCAN box, KRAB domain and the zinc-finger region are indicated

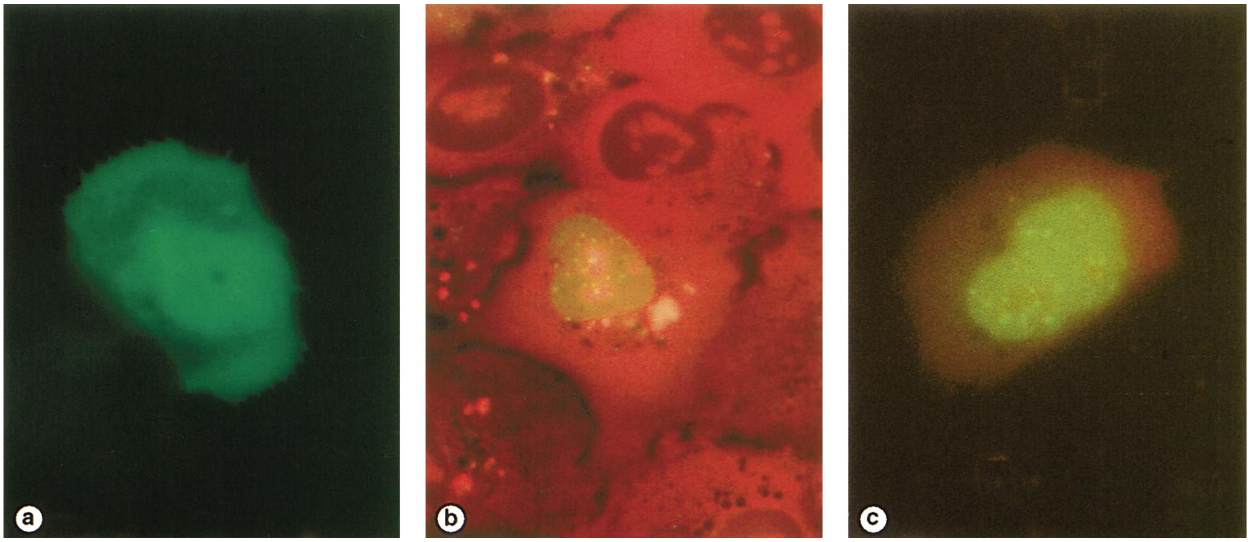

Figure 5 Subcellular localization of *ZNF214* and *ZNF215* Hep3b cells transfected with the empty pEGFPC1 vector (*a*), the GFP-*ZNF214* (*b*), and GFP-*ZNF215* (*c*) fusion proteins. Staining of GFP alone is seen throughout the whole cell. *ZNF214* and *ZNF215* are transported to the nucleus and display a speckled pattern of staining.

staining throughout the whole cell (fig. 5). We note a speckled pattern of staining in the nucleus, excluding the nucleoli, which might indicate that the proteins are present in specific nuclear bodies or domains.

Genomic Imprinting

The molecular etiology of BWS clearly involves imprinting and loss of imprinting control, but there is no a priori reason to suggest that genes at *BWSCR2* need to be imprinted, although both translocations in this region are maternally inherited. Nevertheless, we tested *ZNF215* and *ZNF214* to determine whether this was the case. We screened DNA of 10 normal fetuses and their mothers for polymorphic sites in both genes.

An A→G change at position 355 was identified in *ZNF215*. Two fetuses were heterozygous for this polymorphism while their mothers were homozygous. RNA isolated from different tissues of these two fetuses was used to determine allelic expression patterns of variants *ZNF215V1* and *ZNF215V3*. SSCP analysis of appropriate RT-PCR products of *ZNF215V1* and *ZNF215V3* (fig. 6a, b, c, d) shows that the maternal allele of *ZNF215V1* is preferentially expressed in liver, lung, kidney, and testis but also that, in the brain and heart, these alleles are nearly equally expressed. Interestingly, *ZNF215V3* also is partially imprinted in lung, liver, and kidney but is completely imprinted in heart. In brain tissue, however, complete imprinting is seen in fetus 2, whereas, in fetus 1, both alleles are expressed—indicating either that, at least in this tissue, individual variation exists or that imprinting may vary in different stages of development (developmental stages of the fetuses used are not known). A summary of the results is shown in table 1.

In *ZNF214*, we found a polymorphism at position 383 (T→G and T→A). Sequencing analysis of appropriate RT-PCR products of *ZNF214* showed that both alleles are expressed at roughly equal intensities in heart, lung, brain, and liver, indicating that *ZNF214* is not imprinted.

Table 1

Summary of Imprinting of *ZNF215V1* and *ZNF215V3*

Fetus and Tissue	*ZNF215V1*	*ZNF215V3*
1f:		
Heart	M >/≈ P	M
Lung	M > P	M > P
Kidney	M > P	ND
Testis	M > P	ND
Brain	M ≈ P	M >/≈ P
2f:		
Heart	ND	M
Liver	M > P	M > P
Kidney	M > P	M > P
Brain	M ≈ P	M

NOTE.—M ≈ P, equal expression maternal and paternal alleles; M > P, preferential expression of the maternal allele; M, expression almost exclusively from the maternal allele; M >/≈ P, roughly equal expression slightly favoring the maternal allele; ND, not done.

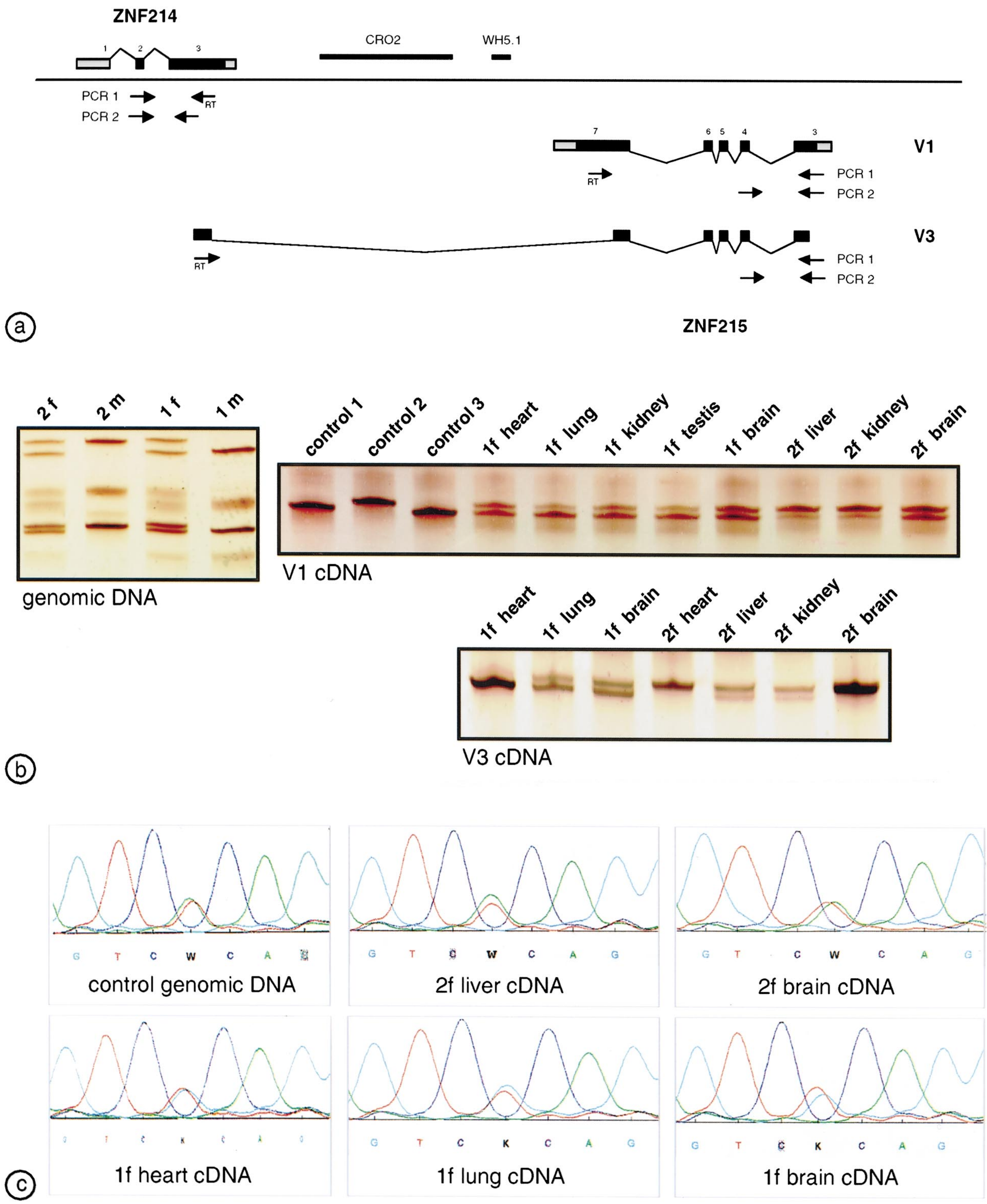

Figure 6 Genomic imprinting of *ZNF215*. *a,* Schematic overview of the primers used for amplification of *ZNF214* and *ZNF215V1* and *ZNF215V3*. RT indicates primers used for reverse transcription. *b,* SSCP of *ZNF215* genomic and cDNA. Both fetuses (1f and 2f) are heterozygous, whereas their mothers (1m and 2m) are homozygous. SSCP analysis of *ZNF215V1* cDNA derived from different tissues of 1f and 2f homozygous control samples.shows that both alleles are expressed, although the maternal allele is more abundantly expressed in all tissues except brain and heart. SSCP analysis of *ZNF215V3* cDNA shows that expression is predominantly from the maternal allele in lung, liver, kidney, and brain of 1f. Expression is exclusively from the maternal allele in heart and brain of 2f. *c,* Sequence analysis of *ZNF214* on genomic heterozygous DNA and RT-PCR products of *ZNF214* derived from different tissues of 1f and 2f shows no indication for imprinting.

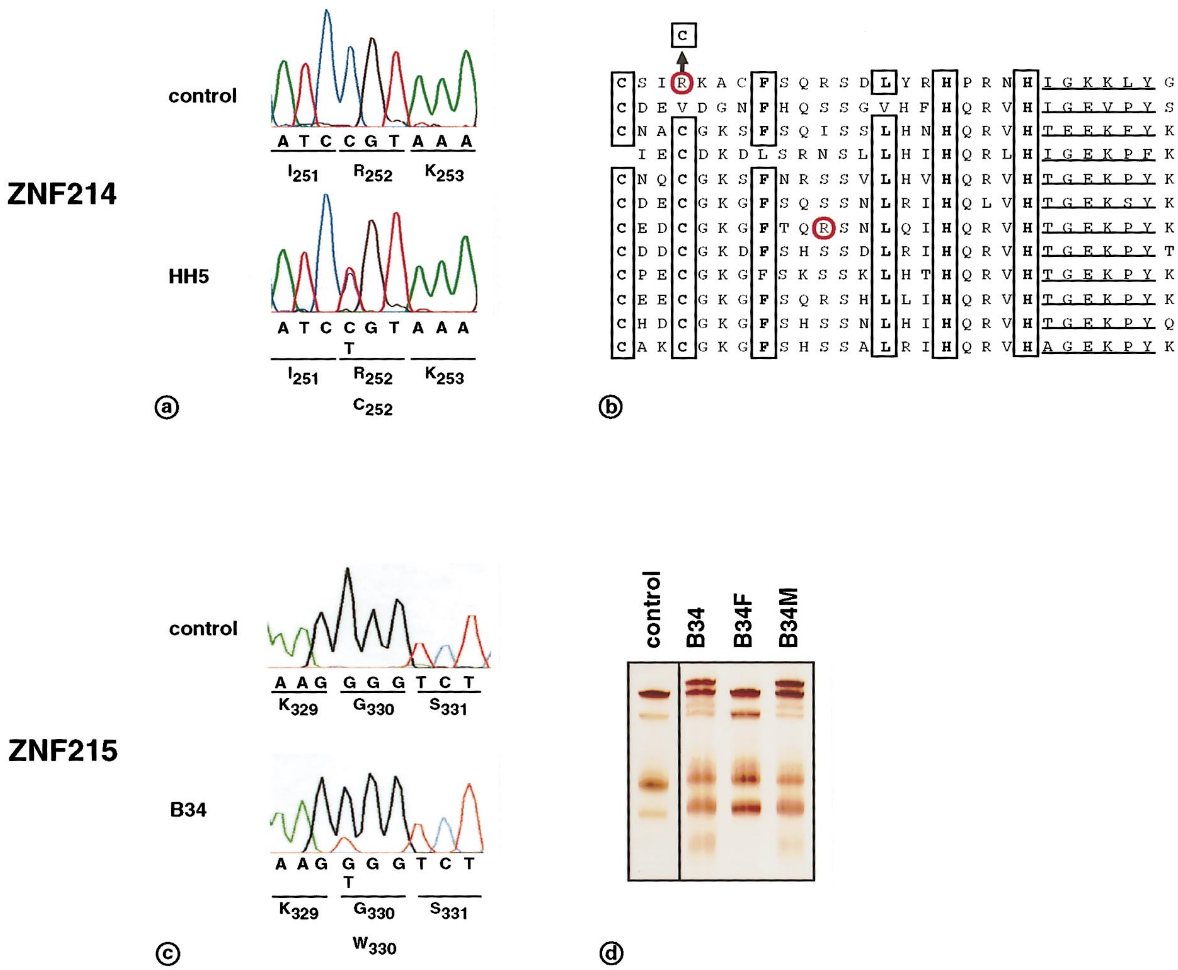

Figure 7 Variations in *ZNF214* and *ZNF215*. *a,* Sequence analysis of *ZNF214* in patient HH5, who has the R252C variant, and a control individual. *b,* Alignment of the twelve zinc fingers of *ZNF214*. The amino acids of the conserved zinc-finger consensus sequence are indicated. The variable sites are indicated with red circles. The *R252C* variant restores the first imperfect zinc-finger, and the *R426H* is in the seventh zinc-finger. *c,* Sequence analysis of *ZNF215* in patient B34 and a control individual. *d,* SSCP pattern of fragment 8 of *ZNF215* from patient B34, her father (B34F) and her mother (B34M). The variant is inherited from the mother.

Mutational Analysis

Only two chromosomal rearrangements define *BWSCR2*. If either or both of *ZNF214* and *ZNF215* do indeed play a role in BWS, then we might expect mutations to be found in these genes in at least a subset of cytologically unaltered BWS patients. To search for these, we set up an SSCP strategy to screen for mutations in both genes in 32 patients with BWS and 11 patients with isolated hemihypertrophy (all non-UPD cases). In *ZNF214,* we found a 754C→T change in 6 of 44 patient samples (2 from patients with BWS, 2 from patients with BWS with hemihypertrophy, and 2 from patients with isolated hemihypertrophy), compared to 2 of 205 control individuals (significant at $P < .01$). This change results in an arginine-to-cysteine conversion in the first finger and restores this normally imperfect finger (fig. 7b). In addition a 1277G→A change, leading to a R426H substitution in the seventh zinc-finger, was found in a single patient (fig. 7b). This alteration is inherited from the presumably unaffected father.

In *ZNF215,* a 988G→T transition was found in 1 patient with BWS (fig. 7c, d). This variant was also found in the mother of the patient and was not present in 48 control individuals. The transition changes a glycine to a tryptophan in a potential phosphorylation site (RKGS).

Discussion

In this study, we set out to test the hypothesis that there could be a gene(s) located at the *BWSCR2* region that could contribute to the BWS phenotype. The two chromosomal rearrangements that define *BWSCR2* both disrupt the zinc-finger gene *ZNF215,* thus meeting the first formal requirement for any gene's involvement in the etiology of BWS—that it must be disrupted by the rearrangements.

The breakpoints in *BWSCR2* disrupt alternative-spliced *ZNF215* transcripts (*ZNF215V2* and *ZNF215V3*). These transcripts encode a truncated protein lacking the zinc fingers but retaining the KRAB and SCAN box functional domains. KRAB domains are found in about one-third of all C_2H_2-class zinc fingers and transfection experiments have shown that it is able to repress transcription (Margolin et al. 1994; Witzgall et al. 1994). The function of a SCAN box is still unknown but its α-helical structure suggests that it may serve as a dimerization domain (Williams et al. 1995). It is an attractive but speculative hypothesis that, on the basis of their respective protein motifs, *ZNF215V1* is a zinc-finger transcription factor and that *ZNF215V2* and *ZNF215V3* are regulatory proteins. The finding that both *ZNF214* and *ZNF215V1* proteins are transported to the nucleus, as determined by transfection studies using GFP fusion proteins, is compatible with such a role. Alternative-spliced transcripts encoding truncated proteins are also found in some other transcription factors—for example, some members of the *HOX* gene family, whose alternative transcripts encode proteins lacking the homeobox domain (La Rosa et al. 1988; Shen et al. 1991; Hong et al. 1995; Fujimoto et al. 1998). The *ZNF215V2* and *ZNF215V3* alternative-spliced transcripts are partially antisense of *ZNF214,* and it is possible that transcription of *ZNF215V2* and *ZNF215V3* may modulate levels of *ZNF214* transcription or translation.

Although we found some alterations in *ZNF214* and *ZNF215* in patients, we do not have evidence for functional mutations in these genes. The incidence of the 252C allele in *ZNF214* is significantly higher in BWS than in the unaffected population, but its involvement in these diseases cannot yet be considered proven. A more direct test of function will be required to prove a causal relationship. The significance of the single *R426H* variant in *ZNF214* and the *G330W* variant in *ZNF215* is unclear.

The finding that *ZNF215V1* and *ZNF215V3* are imprinted may be significant. Both *BWSCR2* rearrangements are maternally derived suggesting these two patients will harbor an active but rearranged *ZNF215* gene and a paternally derived, unrearranged, but predominantly inactive normal gene.

BWSCR2 appears to be associated with hemihypertrophy, unlike rearrangements of *BWSCR1* or *BWSCR3*. The mouse models of BWS suggest involvement of *CDKN1C* and *IGF2* but fail to account for the presence of hemihypertrophy. The *cdkn1c* null mouse develops some BWS features such as omphalocoele and other abdominal-wall defects, but no overgrowth (Zhang et al. 1997; Yan et al. 1997). The *Igf2* transgenic mouse shows gigantism and organomegaly (Sun et al. 1997). Together, these mice account for a large proportion of BWS features, but not hemihypertrophy. It has been suggested that mosaic UPD causes the local hypertrophy, but chimaeric transgenic *Igf2* mice do not show this and the translocations involving *BWSCR2* are constitutional. It is possible that hypertrophy is the product of a local stochastic event (possibly *IGF2* activation) that can be largely asymmetric (hemihypertrophy) or largely symmetric (organomegaly). Evidence for this hypothesis does not yet exist and will require a proper understanding of the functions of the ZNF214 and ZNF215 proteins.

Acknowledgments

Work in MMAMM's lab was supported by The Netherlands Organization of Scientific Research (NWO grant 504-111) and by the European Community, Biomed2 project BMH4-CT96-1428. Work in PFRL's lab was supported by grants from the United Kingdom Medical Research Council, the European Community (see above), and the Wellcome Trust. Work in APF's lab was supported by NIH grant CA54358. Cosmids q25 and q27 were sequenced by Paul Matthews and Amanda McMurray at the Sanger Centre, Hinxton, supported by the Wellcome Trust. We would like to thank P. K. Nieuwenhuisen and G. Salieb-Beugelaar for their contribution and technical assistance.

Electronic-Database Information

Accession numbers and URLs for data in this article are as follows:

Genbank, http://www.ncbi.nlm.gov (for accession numbers of q27 [Z68746], q25 [Z68344], *ZNF214* [AF056617] and *ZNF215* [AF056618])

Online Mendelian Inheritance in Man (OMIM), http://www.ncbi.nih.gov/Omim (for BWS [MIM 130650] and WT2 [MIM 194071])

United Kingdom MRC Human Genome Project Resource Centre, http://www.hgmp.mrc.ac.uk/

References

Brown KW, Villar AJ, Bickmore W, Clayton-Smith J, Catchpoole D, Maher ER, Reik W (1996) Imprinting mutation in the Beckwith-Wiedemann syndrome leads to biallelic *IGF2* expression through an H19-independent pathway. Hum Mol Genet 5:2027–2032

DeBaun MR, Tucker M (1998) Risk of cancer during the first four years of life in children from the Beckwith-Wiedemann Syndrome Registry. J Pediatr 132:398–400

Eggenschwiler J, Ludwig T, Fisher P, Leighton PA, Tilghman SM, Efstratiadis A (1997) Mouse mutant embryos overexpressing Igf-II exhibit phenotypic features of the Beckwith-Wiedemann and Simpson-Golabi-Behmel-Syndromes. Genes Dev 11:3128–3142

Fidlerova H, Senger G, Kost M, Sanseau P, Sheer D (1994) Two simple procedures for releasing chromatin from routinely fixed cells for fluorescence in situ hybridization. Cytogenet Cell Genet 65:203–205

Fujimoto S, Araki K, Chisaki O, Araki M, Takagi K, Yamamura K (1998) Analysis of the murine hoxa-9 cDNA: an alternatively spliced transcript encodes a truncated protein lacking the homeodomain. Gene 209:77–85

Hatada I, Ohashi H, Fukushima Y, Kaneko Y, Inoue M, Komoto Y, Okada A, et al (1996) An imprinted gene *p57*^{KIP2} is mutated in Beckwith-Wiedemann syndrome. Nat Genet 14:171–173

Hong YS, Kim SY, Bhattacharya A, Pratt DR, Hong WK, Tainsky M (1995) Structure and function of the HOX A1 human homeobox gene cDNA. Gene 159:209–214

Hoovers JM, Kalikin LM, Johnson LA, Alders M, Redeker B, Law DJ, Bliek J, et al (1995) Multiple genetic loci within 11p15 defined by Beckwith-Wiedemann syndrome rearrangement breakpoints and subchromosomal transferable fragments. Proc Natl Acad Sci USA 92:12456–12460

Hoovers JM, Mannens M, John R, Bliek J, van Heyningen V, Porteous DJ, Leschot NJ, et al (1992) High-resolution localization of 69 potential human zinc- finger protein genes: a number are clustered. Genomics 12:254–263

Ivens AC, Little PFR (1994) Cosmid clones and their application to genome studies. In: Glover D (ed) DNA cloning—complex genomes: a practical approach. IRL Press, Oxford, pp 1–47

Joyce JA, Lam WK, Catchpoole DJ, Jenks P, Reik W, Maher ER, Schofield PN (1997) Imprinting of *IGF2* and *H19*—lack of reciprocity in sporadic Beckwith-Wiedemann-Syndrome. Hum Mol Genet 6:1543–1548

Koufos A, Grundy P, Morgan K, Aleck KA, Hadro T, Lampkin BC, Kalbakji A, et al (1989) Familial Wiedemann-Beckwith syndrome and a second Wilms tumor locus both map to 11p15.5. Am J Hum Genet 44:711–719

La Rosa GJ, Gudas LJ (1988) Early retinoic acid induced F9 teratocarcinoma stem cell gene ERA-1: alternative splicing creates transcripts for a homeobox-containing protein and one lacking the homeobox. Mol Cell Biol 8:3906–3917

Lee MP, Debaun M, Randhawa G, Reichard BA, Elledge SJ, Feinberg AP (1997*a*) Low frequency of *p57*(*kip2*) mutation in Beckwith-Wiedemann-Syndrome. Am J Hum Genet 61: 304–309

Lee MP, Hu RJ, Johnson LA, Feinberg AP (1997*b*) Human *KVLQT1* gene shows tissue-specific imprinting and encompasses Beckwith-Wiedemann syndrome chromosomal rearrangements. Nat Genet 15:181–185

Mannens M, Hoovers JM, Redeker E, Verjaal M, Feinberg AP, Little P, Boavida M, et al (1994) Parental imprinting of human chromosome region 11p15.3-pter involved in the Beckwith-Wiedemann syndrome and various human neoplasia. Eur J Hum Genet 2:3–23

Margolin JF, Friedman JR, Meyer WK, Vissing H, Thiesen HJ, Rauscher FJ 3d (1994) Kruppel-associated boxes are potent transcriptional repression domains. Proc Natl Acad Sci USA 91:4509–4513

Okeefe D, Dao D, Zhao L, Sanderson R, Warburton D, Weiss L, Anyaneyeboa K, et al (1997) Coding mutations in *p57*(*kip2*) are present in some cases of Beckwith-Wiedemann-Syndrome but are rare or absent in Wilms tumors. Am J Hum Genet 61:295–303

Pettenati MJ, Haines JL, Higgins RR, Wappner RS, Palmer CG, Weaver DD (1986) Wiedemann-Beckwith syndrome: presentation of clinical and cytogenetic data on 22 new cases and review of the literature. Hum Genet 74:143–154

Ping AJ, Reeve AE, Law DJ, Young MR, Boehnke M, Feinberg AP (1989) Genetic linkage of Beckwith-Wiedemann syndrome to 11p15. Am J Hum Genet 44:720–723

Redeker E, Alders M, Hoovers JM, Richard CW 3rd, Westerveld A, Mannens M (1995) Physical mapping of 3 candidate tumor suppressor genes relative to Beckwith-Wiedemann syndrome associated chromosomal breakpoints at 11p15.3. Cytogenet Cell Genet 68:222–225

Redeker E, Hoovers JM, Alders M, van Moorsel CJ, Ivens AC, Gregory S, Kalikin L, et al (1994) An integrated physical map of 210 markers assigned to the short arm of human chromosome 11. Genomics 21:538–550

Reik W, Brown KW, Schneid H, Le Bouc Y, Bickmore WX, Maher ER (1995) Imprinting mutations in the Beckwith-Wiedemann syndrome suggested by altered imprinting pattern in the *IGF2-H19* domain. Hum Mol Genet 4: 2379–2385

Shen WF, Detmer K, Simonitch-Eason TA, Lawrence HJ, Largman C (1991) Alternative splicing of the HOX2.2 homeobox gene in human hematopoietic cells and murine embryonic and adult tissues. Nucleic Acids Res 19:539–545

Smilinich NJ, Day CD, Fitzpatrick GV, Caldwell GM, Lossie AAC, Cooper PR, Smallwood AC, et al (1999) A maternally methylated CpG island in KvLQT1 is associated with an antisense paternal transcript and loss of imprinting in Beckwith-Wiedemann syndrome. Proc Natl Acad Sci USA 96: 8064–8069

Sun FL, Dean WL, Kelsey G, Allen ND, Reik W (1997) Transactivation of *IGF2* in a mouse model of Beckwith-Wiedemann syndrome. Nature 389:809–815

Weksberg R, Shen DR, Fei YL, Song QL, Squire J (1993) Disruption of insulin-like growth factor 2 imprinting in Beckwith-Wiedemann syndrome. Nat Genet 5:143–150

Weksberg R, Squire J (1996) Molecular biology of Beckwith-Wiedemann syndrome. Med Pediatr Oncol 27:462–469

Wiedemann HR (1983) Tumours and hemihypertrophy associated with Wiedemann-Beckwith syndrome. Eur J Pediatr 141:129

Williams AJ, Khachigian LM, Shows T, Collins T (1995) Isolation and characterization of a novel zinc-finger protein with transcription repressor activity. J Biol Chem 270: 22143–22152

Witzgall R, O'Leary E, Leaf A, Onaldi D, Bonventre JV (1994) The Kruppel-associated box-A (KRAB-A) domain of zinc-finger proteins mediates transcriptional repression. Proc Natl Acad Sci USA 91:4514–4518

Yan Y, Frisen J, Lee MH, Massague J, Barbacid M (1997)

Ablation of the CDK inhibitor *p57Kip2* results in increased apoptosis and delayed differentiation during mouse development. Genes Dev 11:973–983
Zhang PM, Liegeois NJ, Wong C, Finegold M, Hou H, Thompson JC, Silverman A, et al. (1997) Altered cell differentiation and proliferation in mice lacking p57(kip2) indicates a role in Beckwith-Wiedemann-Syndrome. Nature 387:151–158